For crystalline polymers the main term of interest outside the zero order scatter will be I_B. Equation (3) has, therefore, been evaluated in part II (Blundell, 1970) for the particular case when $\xi(y)$ has a trapezium-like profile. This case represents a structure whose projected density shows a gradual linear change in density on going from the amorphous to the crystalline values.

The author wishes to thank Dr A. Keller and Dr E. R. Howells for their encouragement to write these papers.

References

BLUNDELL, D. J. (1970). *Acta Cryst.* A**26**, 476.
BONART, R. (1966). *Kolloid-Z.* **211**, 14.
GUINIER, A. (1963). *X-ray Diffraction in Crystals, Imperfect Crystals and Amorphous Bodies*. San Francisco: Freeman.
HERMANS, J. J. (1944). *Rec. Trav. Chim. Pays-Bas*, **63**, 211.
HOSEMANN, R. (1949). *Z. Phys.* **127**, 16.
HOSEMANN, R. & BAGCHI, S. N. (1962). *Direct Analysis of Diffraction by Matter*. Amsterdam: North Holland.
KELLER, A. (1968). *Reports Progr. Phys.* **31**, 623.
KORTLEVE, G. & VONK, C. G. (1968). *Kolloid-Z.* **225**, 124.
VONK, C. G. & KORTLEVE, G. (1967). *Kolloid-Z.* **220**, 19.
ZERNIKE, F. & PRINS, J. A. (1927). *Z. Phys.* **41**, 184.

Acta Cryst. (1970). A**26**, 476

One-Dimensional Models for Small-Angle X-ray Diffraction from Crystalline Polymers. II. Model with Continuous Density Changes between Phases

BY D. J. BLUNDELL

Imperial Chemical Industries Limited, Petrochemical and Polymer Laboratory, P.O. Box 11, *The Heath, Runcorn, Cheshire, England*

(*Received* 11 *September* 1969)

The small angle X-ray scatter from crystalline polymers is evaluated by using a one-dimensional model where the density between crystal and amorphous phases changes linearly over a finite transition range t, and where the sizes of the crystal and amorphous regions fluctuate according to independent Gaussian distributions. The calculation is based on the general model formulated in part I. Approximate expressions are derived for the width and area of the diffraction peaks. The dependence on t occurs in the factor $\sin^2 \pi st/(\pi st)^2$ which affects only the peak intensities. An analysis is made to find how the factor will modify theoretical interpretations based on experimental intensity measurements.

1. Introduction

When X-rays are scattered from crystalline polymers, diffraction maxima are observed at small angles corresponding to Bragg spacings of a few hundred Ångströms. This scatter is generally attributed to an alternation in texture between crystalline and amorphous-like intercrystalline regions, in which both regions fluctuate in thickness about their respective mean values. Most theoretical treatments consider the phenomenon in terms of one-dimensional models where the mean density changes abruptly between the crystalline and amorphous values, giving a rectangular step density profile. The model discussed in this article introduces, between each phase, a transition zone where there is linear change in density from the crystalline to amorphous value, thus giving a repeated trapezium shape to the density profile.

The review of the basic scattering situation in part I (Blundell, 1970) showed that the periodicity within a typical polymer sample can be represented by a one-dimensional model consisting of a line of non-overlapping scattering rods arranged parallel to the periodicity. The line of rods can then be interpreted as representing the projection onto the line of the excess in electron density over the background amorphous value. Part I concluded by formulating a general expression for the scattered intensity of a model where the density along a rod was given by an arbitrary function ξ. In the present work ξ is taken to have a trapezium profile in which there are transition zones of length t at the ends of each rod. Such a transition length has also been considered by Tsvankin (1964 *a*, *b*) in a model which is based on slightly different assumptions from those used in part I, and which employed different distribution statistics from those used here. However in Tsvankin's conclusions, the effects of t are not clearly resolved from the other parameters in his model. In the present article particular attention is paid to the ways in which the intensity curves for a simple rectangle profile must be modified when a transition zone is introduced.

In this article particular reference is made to the conditions prevailing in samples made by sedimenting solution grown crystals (particularly polyethylene), since of all polymer systems these have the most well char-

acterized morphology. In their simplest form, polymer crystals are single lamellae about 100 Å thick. In the interior the polymer chains are arranged approximately perpendicular to the plane of the lamellae. On reaching the planar surfaces of the lamellae, most of the chains fold back into the crystal. It would appear that some of the folds are sharp and regular. The remaining looser folds together with free chain ends form layers about 10 Å thick on the lameller faces where the density approaches that of amorphous polymer (Keller, 1968). Because of the complicated nature of the fold surface it is difficult to define the precise boundary of the regions possessing the crystalline density. On the fine scale the boundary can meander according to the size and configuration of each individual fold. On the larger scale the boundary will follow any fluctuation in crystalline thickness resulting from the chain folding crystallization process (Frank & Tosi, 1961). Apart from the crystalline regions, fluctuations possibly of a related kind can also take place in the nature of the surface layers (Bassett, Blundell & Keller, 1967). The total thickness of the lamellae will exhibit a fluctuation which is the combined effect of the fluctuations in the crystalline and disordered surface regions. On sedimenting and drying to form samples for diffraction studies, the crystals stack together to give periodic one-dimensional crystal–amorphous structures running at right angles to the lamellar planes. The need to examine the effect of a transition zone becomes apparent when one considers the projection of the mean electron density onto a line perpendicular to the lamellae. To a first approximation one will obtain the rectangle profile discussed previously by other authors. However such a representation cannot be wholly realistic since one would expect the projection of a meandering boundary to produce more gradual changes in density. As a better approximation one is therefore led to introduce a transition zone where there is a linear change in density. It should be noted that several three-dimensional structures can give rise to this one-dimensional model. There is no way of distinguishing whether the transition zone is the result of a gradual density change on an atomic level or whether it reflects the projection on a larger scale of a meandering sharp crystal–amorphous boundary. (The problem is complex and depends on knowing the lateral extent over which the projection procedure should be performed. The findings of Hosemann, Wilke & Balta Calleja (1966) suggest that the projection should be limited to lateral domains only a few hundred Ångströms wide.) In order to include all reasonable possibilities in the case of a meandering boundary, transition lengths approaching the mean amorphous thickness should be considered. Thus for polyethylene crystals where the crystalline regions typically occupy about 80% of total lamellar thickness, one would need to examine a range of t up to at least 15% of total thickness. Although the transition zone can reflect boundary fluctuations within a given lamella, one must in a trapezium model still allow the lengths of the rods and gaps to fluctuate statistically in order to account for fluctuations between different layers. Previous experiments with polyethylene crystals (Hosemann, 1967; Williams, Blundell, Keller & Ward, 1968) suggest that in the model one should consider fluctuations with standard deviations of about 10% of mean thickness, or less. In the more complicated bulk crystallized polymer, the deviation will be significantly greater.

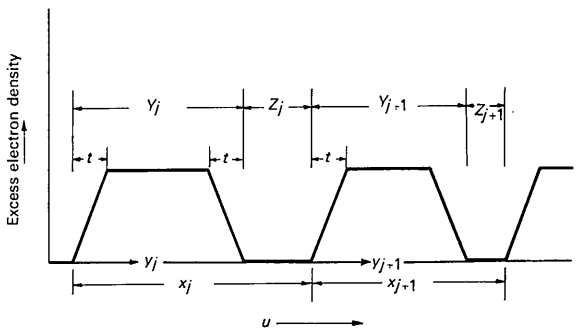

Fig. 1. Model of scattering rods with trapezium density profile.

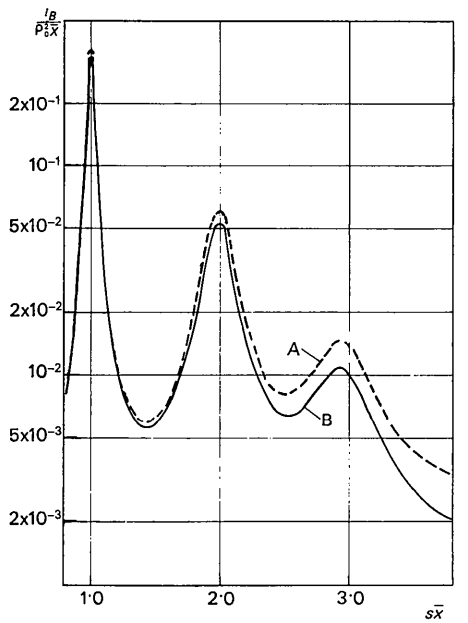

Fig. 2. I_B calculated from equation (1) with $\chi=0{\cdot}8$, $\sigma_x=0{\cdot}1\bar{X}$, $\sigma_y/\bar{Y}=\sigma_z/\bar{Z}$; curve A, $t=0$; curve B, $t=0{\cdot}1\bar{X}$.

The discussion of the trapezium profile model is in four parts. First an intensity expression is evaluated using the results of part I. Then the shape and variation of the intensity curve is related qualitatively with the variable parameters of the model. Next approximate expressions are developed which describe the area and width of the diffraction peaks in terms of the model parameters. Finally these expressions are discussed in relation to typical experimental measurements, with particular reference to the way a transition zone can modify the deductions.

2. Trapezium model

The general profile model considered in part I consists of N scattering rods denoted individually by the subscript j arranged along a u axis. Fig. 1 shows the corresponding representation of the density variation for rods with trapezium profiles. For the jth rod, which is of length Y_j the density along its length is given by

$$\begin{aligned}\xi(y_j) &= \frac{\varrho_0 y_j}{t} && \text{for} \quad 0 \le y_j \le t \\ &= \varrho_0 && \text{for} \quad t < y_j \le (Y_j - t) \\ &= \varrho_0 (Y_j - y_j)/t && \text{for} \quad (Y_j - t) < y_j \le Y_j .\end{aligned}$$

In the present model, the transition distance t at the rod ends will be taken to be a constant for all rods. ϱ_0 will be taken to be the difference $\varrho_C - \varrho_A$ between the mean electron densities of the crystalline and amorphous-like regions. The general model is based on the premise that there is no correlation between the fluctuation statistics $H(Y_j)$ of the rod lengths Y_j, and the statistics $h(Z_j)$ of the gap lengths Z_j. For analytical convenience $H(Y_j)$ and $h(Z_i)$ will here be taken to be symmetrical Gaussian distributions, and will be defined by

$$H(Y_j) = \frac{1}{\sigma_y \sqrt{2\pi}} \exp\left\{\frac{-(Y_j - \bar{Y})^2}{2\sigma_y^2}\right\}$$

and

$$h(Z_j) = \frac{1}{\sigma_z \sqrt{2\pi}} \exp\left\{\frac{-(Z_j - \bar{Z})^2}{2\sigma_z^2}\right\}$$

where $\bar{Y}$ and $\bar{Z}$ are the respective mean lengths of the rods and gaps, and σ_y and σ_z are the respective standard deviations. A survey of models where H and h are various symmetrical distributions has shown that essentially identical results will be obtained for any reasonable symmetric functions of corresponding width to the above Gaussian distributions. If, however, assymmetric distributions are used for H and h, the shape of the diffraction peaks will be distorted accordingly (Rheinhold, Fischer & Peterlin, 1964; Kortleve & Vonk, 1968). In the particular case of solution grown crystals there has been no evidence of asymmetry. The volume crystallinity χ of the structure represented by the above trapezium rods will be

$$\chi = \frac{\bar{Y} - t}{\bar{X}}$$

where $\bar{X} = \bar{Y} + \bar{Z}$ is the mean periodic distance.

In part I, the scattered intensity was shown to consist of two terms I_B and I_C, where I_B was directly proportional to N. In this article the straightforward case will be considered where N is sufficiently large that I_C can be neglected in the region of interest. Using the above definitions of ξ, H and h it is found that the main component I_B per unit volume of scatterer reduces to

$$I_B(s) = \frac{\varrho_0^2}{2\pi^2 s^2 \bar{X}} \left\{\frac{\sin^2 \pi s t}{(\pi s t)^2}\right\} \times \left\{\begin{array}{c} 1 - |F_x|^2 - |F_y|\,(1 - |F_z|^2) \cos 2\pi s \chi \bar{X} \\ - |F_z|\,(1 - |F_y|^2) \cos 2\pi s (1 - \chi) \bar{X} \\ |1 - F_x|^2 \end{array}\right\} \quad (1)$$

where

$$\begin{aligned} F_y &= \exp(-2\pi^2 s^2 \sigma_y^2) \exp(-2\pi i s \bar{Y}) \\ F_z &= \exp(-2\pi^2 s^2 \sigma_z^2) \exp(-2\pi i s \bar{Z}) \\ F_x &= \exp(-2\pi^2 s^2 [\sigma_y^2 + \sigma_z^2]) \exp(-2\pi i s [\bar{Y} + \bar{Z}]) , \end{aligned}$$

so that

$$\begin{aligned} |F_y| &= \exp(-2\pi^2 s^2 \sigma_y^2) \\ |F_z| &= \exp(-2\pi^2 s^2 \sigma_z^2) \\ |F_x| &= \exp(-2\pi^2 s^2 [\sigma_y^2 + \sigma_z^2]) . \end{aligned}$$

The total angle of scatter 2θ is derived from the variable

$$s = \frac{2 \sin \theta}{\lambda} .$$

By putting

$$\sigma_x^2 = \sigma_y^2 + \sigma_z^2 \quad (2)$$

it can be seen that F_x is related to the fluctuation of the total period $\bar{X}$ in the same way that F_y and F_z are related to $\bar{Y}$ and $\bar{Z}$, and that σ_x is the standard deviation of the periodic lengths about the mean $\bar{X}$.

3. Relation between intensity curve and model parameters

3.1. *General form of* I_B

Typical forms of equation (1) are shown in Figs. 2, 3, 4 and 5, where I_B is plotted against the variable $s\bar{X}$.

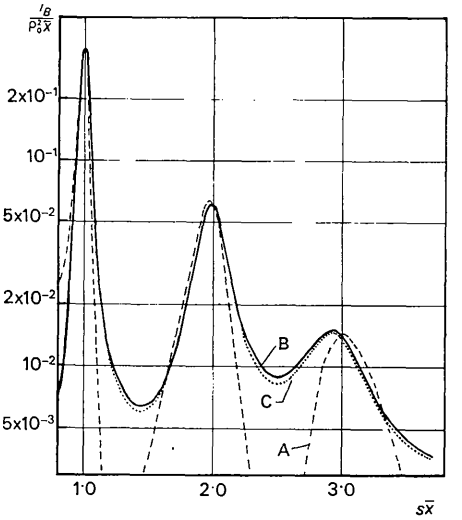

Fig. 3. I_B calculated from equation (1) with $\chi = 0{\cdot}8$, $t = 0$ and where σ_y and σ_z are varied keeping $\sigma_x = 0{\cdot}1\bar{X}$; curve A, $\sigma_y = 0$, $\sigma_z = 0{\cdot}5\bar{Z}$; curve B, $\sigma_y = 0{\cdot}125\bar{Y}$, $\sigma_z = 0$; curve C, $\sigma_y = 0{\cdot}121\bar{Y}$, $\sigma_z = 0{\cdot}121\bar{Z}$.

The increase in width of the diffraction peaks with increasing order is typical of periodic structures where long-range order is destroyed. The maxima appear close to positions where $s\bar{X}$ is integral. Since $s = 2\sin\theta/\lambda$, this is consistent with Bragg's Law (Hosemann, 1949). This well known fact is used regularly to estimate the mean periodic length $\bar{X}$. Distortions from true Bragg positions can occur when the peaks are broad (Lindenmeyer & Hosemann, 1963) or if H or h are asymmetric (Rheinhold, Fischer & Peterlin, 1964), but this is not the concern of this article.

It should be noted that I_B gives no zero order scatter and approaches zero for $s\bar{X} < 1$. The zero order scatter for the model is contained in the neglected I_C (part I; Hosemann & Bagchi, 1962, p. 419).

3.2. *Influence of t*

The parameter t which is of particular interest is isolated in the simple factor $\sin^2\pi st/(\pi st)^2$. When $t \to 0$, this factor approaches unity and one obtains the degenerate rectangle profile. The form of the factor is familiar. As st increases from zero, the factor decreases and then oscillates positively with decreasing amplitude, going through zero at integral values of st. Since for polymers we are only interested in $t \lesssim 0{\cdot}15\ \bar{X}$ and in the intensity curve for $s\bar{X} \lesssim 5$, we will only be concerned with the initial fall-off from unity.

The scatter for a trapezium profile can therefore be regarded as being identical to that of the rectangle profile of equivalent crystallinity, but modified by the slowly decreasing $\sin^2\pi st/(\pi st)^2$ factor.* The influence of the factor becomes increasingly effective with higher scattering angles and is illustrated in Fig. 2.

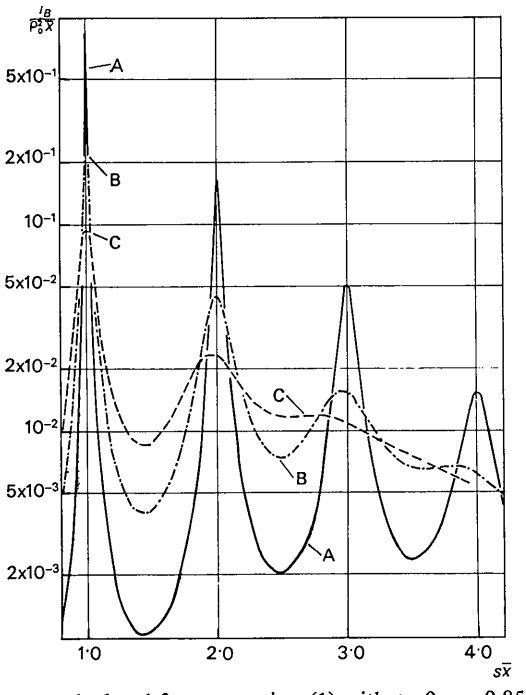

Fig. 4. I_B calculated from equation (1) with $t=0$, $\chi=0{\cdot}85$ and where σ_x is varied, keeping $\sigma_y/\bar{Y} = \sigma_z/\bar{Z}$; curve A, $\sigma_x = 0{\cdot}05\bar{X}$; curve B, $\sigma_x = 0{\cdot}1\bar{X}$; curve C, $\sigma_x = 0{\cdot}15\bar{X}$.

3.3 *Combinations of σ_y and σ_z for given σ_x*

According to equation (2), there is a whole range of combinations of the individual deviations σ_y and σ_z that can produce the same overall σ_x. The range is illustrated by Fig. 3, which shows I_B calculated from (1) for three cases in which $\sigma_x = 0{\cdot}1\ \bar{X}$. Curve A is for one extreme where $\sigma_y = 0$ and the fluctuations occur only in the gap lengths. Curve B is for the other extreme where $\sigma_z = 0$. Curve C is the particular intermediate case where $\sigma_y/\bar{Y} = \sigma_z/\bar{Z}$. For these curves χ has the relatively high value of 0·8, so that $\bar{Z} \ll \bar{Y}$. Therefore for curve C, $\sigma_z \ll \sigma_y$ and hence the curve is almost coincident with B where $\sigma_z = 0$.

Bearing in mind the logarithmic scale, it is important to note that the main features such as peak height and width are essentially the same in all three cases, especially for the well-resolved peaks. The main discrepancies between the three curves occur in the regions between peaks. With present low-angle X-ray techniques the intensity in these regions would probably be so low that differences between the curves would not be significant. Thus for most practical purposes, any combination of σ_y and σ_z for a given σ_x can be adequately represented by either of the simplified extreme cases illustrated by curves A and B.

3.4. *Separation of σ_x from χ*

The effects of σ_x and χ on I_B are shown in Figs. 4 and 5 which give two series of curves where $\sigma_y/\bar{Y} = \sigma_z/\bar{Z}$, and $t=0$. In Fig. 4 σ_x is varied keeping χ constant at 0·85, and in Fig. 5 χ is varied with σ_x constant at $0{\cdot}075\ \bar{X}$.

For any general combination of σ_y and σ_z, the dependence on σ_x and χ in equation (1) cannot be separated analytically. However according to § 3.3 one is justified in taking the case where $\sigma_z = 0$ as an approximation for the general case. (For high crystallinities – *i.e.* $\chi > 0{\cdot}5$ – this will be better than taking $\sigma_y = 0$, since, in the absence of any evidence to the contrary, it is most probable that individual deviations will be proportional to their respective means. In such cases $\sigma_z \ll \sigma_y$.) If $\sigma_z = 0$, equation (1) reduces to

$$I_B = \bar{X}Q_0^2 \left\{ \frac{\sin^2\pi(1-\chi)s\bar{X}}{\pi^2 s^2 \bar{X}^2} \right\} \left\{ \frac{\sin^2\pi st}{(\pi st)^2} \right\} \times \left\{ \frac{1-|F_x|^2}{1-2|F_x|\cos 2\pi s\bar{X} + |F_x|^2} \right\}. \quad (3)$$

* The referee has pointed out that this follows when one recognizes that the trapezium model can be derived by folding the equivalent rectangle profile with a stencil rectangle function of height $1/t$ and width t. The Fourier transform of the stencil will be $\sin\pi st/\pi st$. It then follows from part I that the rod scattering amplitude f_j and the intensity I_B can be obtained from the rectangle case by multiplying by $\sin\pi st/\pi st$ and $\sin^2\pi st/(\pi st)^2$ respectively.

The parameters σ_x and χ can now be separated into a particle function (P.F.) and a lattice function (L.F.) which may be grouped as follows:

$$\text{P.F.} = \varrho_0^2 \bar{X} \left\{ \frac{\sin^2 \pi(1-\chi) s\bar{X}}{\pi^2 s^2 \bar{X}^2} \right\} \left\{ \frac{\sin^2 \pi s t}{(\pi s t)^2} \right\} \quad (4)$$

$$\text{and L.F.} = \frac{1-|F_x|^2}{1-2|F_x| \cos 2\pi s\bar{X} + |F_x|^2} \,. \quad (5)$$

P.F. is independent of the fluctuations in the lattice period and depends essentially on the shape of the mean crystalline density profile as described by the parameters χ and t. L.F. is the well known formula of Zernike & Prins (1927). It is illustrated in Fig. 6 for $\sigma_x = 0{\cdot}075\ \bar{X}$ and $0{\cdot}15\ \bar{X}$. (The special case represented by equation (3) which is here regarded as an approximation to (1) can, in fact, be derived directly by using the approach of a one-dimensional paracrystal, where one considers only the fluctuations of the lattice rather than independent fluctuations of both rod and gap lengths – see part I.)

4. Width and area of diffraction peaks

The degenerate case when $t=0$ in the simplified equation (3) has already been analysed to obtain expressions for the width and area of the peaks (Hosemann & Bagchi, 1962). A similar approach can be used for the trapezium case. For $(t/\bar{X}) < 0{\cdot}15$ and $\chi > 0{\cdot}7$ the whole P.F. of equation (4) will vary slowly through the peaks of L.F. As a good approximation therefore, the shape of the peaks of I_B can be taken to be identical to their shape in L.F.; the P.F. will act as a modulating factor which will govern the overall peak intensity.

For well-resolved peaks it can be shown that the area under each peak of L.F. is essentially constant for all values of σ_x and order n, and that when this area is integrated with respect to the variable s it takes the value $1/\bar{X}$. (This can be done by approximating $|F_x|$ to the first two terms of the exponential expansion, and by assuming $|F_x|$ will remain constant over the region of each peak.) For a given order n, there is an inverse relation between the width and height of the peaks such that the area remains constant. If the width is defined as the ratio of area/height, it can be shown from the L.F. (Hosemann & Bagchi, 1962) that

$$\delta = \pi^2 n^2 \frac{\sigma_x^2}{\bar{X}^2} \,, \quad (6)$$

where δ is measured on the scale of $s\bar{X}$. δ refers to the width of the peaks of both L.F. and I_B and is seen to be independent of both t and χ.

A value for the integral intensity of the peaks in I_B can be obtained by multiplying the mean values taken by P.F. over the region of the peaks, by the area $1/\bar{X}$ of the L.F. peaks. Using the value of P.F. taken when $s\bar{X}$ has the integral value n, then from equation (4) the nth order peak will have an integral intensity given by

$$I_n = \int_{\substack{\text{over region} \\ \text{of } n\text{th peak}}} I_B \,.\, \mathrm{d}(s\bar{X}) \simeq \varrho_0^2 \left\{ \frac{\sin^2 \dfrac{\pi n t}{\bar{X}}}{\left(\dfrac{\pi n t}{\bar{X}} \right)^2} \right\} \times \left\{ \frac{\sin^2 \pi n(1-\chi)}{(\pi n)^2} \right\} . \quad (7)$$

(In the context of its derivation, equation (7) is only meaningful when the nth order peak is well resolved;

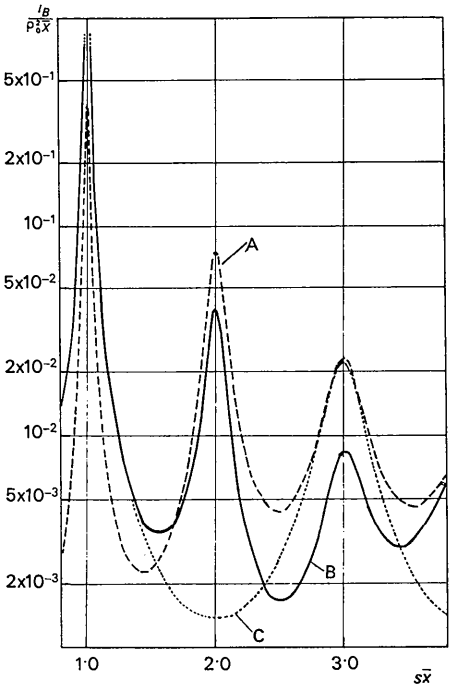

Fig. 5. I_B calculated from equation (1) with $t=0$, $\sigma_x = 0{\cdot}075\bar{X}$ and where χ is varied, keeping $\sigma_y/\bar{Y} = \sigma_z/\bar{Z}$; curve A, $\chi = 0{\cdot}85$; curve B, $\chi = 0{\cdot}6$; curve C, $\chi = 0{\cdot}5$.

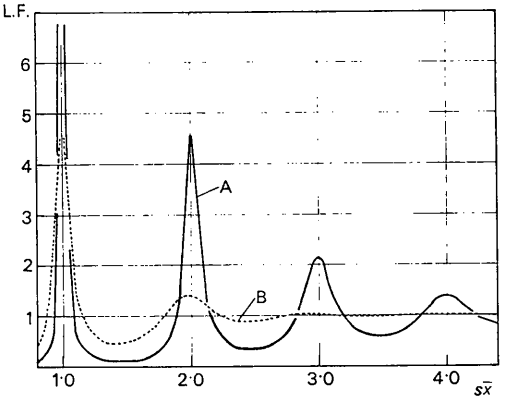

Fig. 6. L.F. calculated from equation (5); curve A, $\sigma_x = 0{\cdot}075\bar{X}$; curve B, $\sigma_x = 0{\cdot}15\bar{X}$.

if this is not so it must be regarded only as an approximation of the integrated intensity over the range $(n-\frac{1}{2})<s\bar{X}<(n+\frac{1}{2})$.)

A useful related quantity is the total integral intensity of I_B over all scattering angles. This can be obtained by the non-rigorous procedure of summing all I_n as given in (7) from orders 1 to infinity. (*N.B.* There is no zero order peak in L.F., nor hence in I_B. All zero order scatter is contained in the neglected intensity component I_C.) Thus the total integrated scatter on one side of the main beam will be

$$\int_0^\infty I_B \cdot \mathrm{d}(s\bar{X}) \simeq \sum_{n=1}^{\infty} I_n = \frac{\varrho_0^2}{2}\left\{\chi(1-\chi)-\frac{t}{3\bar{X}}\right\}. \quad (8)$$

This same relation for $t=0$ has been obtained rigorously by Hosemann & Bagchi (1962) using Jordan's Theorem. The total intensity can also be obtained *via* an alternative route by calculating the mean-square fluctuation $\langle\eta^2\rangle$ of the density (Debye, Anderson & Brumberger, 1957; Porod, 1951, 1952). Equation (8) can be confirmed by calculating $\langle\eta^2\rangle$ for the present trapezium profile.

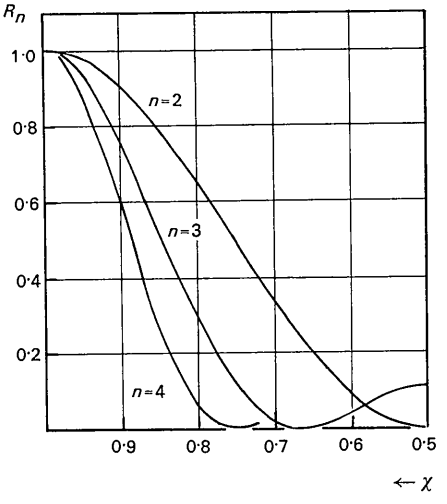

Fig. 7. R_n calculated from equation (9) with $t=0$ and $\chi=0{\cdot}85$.

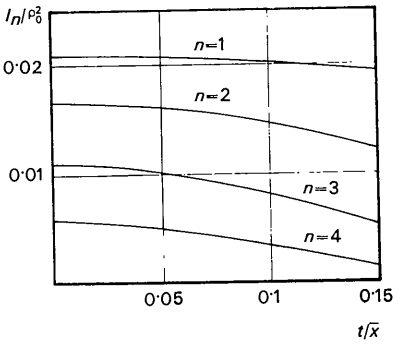

Fig. 8. Variation of I_n with t from equation (7), with $\chi=0{\cdot}85$.

Another useful set of quantities, which is not usually discussed in the literature, is the relative intensities of the different order peaks. Taking the area of the first order peak as the reference standard, the relative integral intensity R_n of the nth order can be defined from equation (7) to be:

$$R_n = \frac{I_n}{I_1} = \frac{1}{n^4}\left\{\frac{\sin^2\pi nt/\bar{X}}{\sin^2\pi t/\bar{X}}\right\}\left\{\frac{\sin^2\pi n(1-\chi)}{\sin^2\pi(1-\chi)}\right\}. \quad (9)$$

Although the expressions (6) to (9) are derived from the simplified case where $\sigma_z=0$ and have also involved several further approximations, good agreement is found with measurements made directly on curves calculated from the full equation (1). The agreement can be seen qualitatively from the examples in Figs. 4 and 5. The quantity R_n shown plotted in Fig. 7 for $t=0$ checks with the behaviour of these curves. Fig. 8 shows the effect of t on I_n keeping χ constant. The influence of the $\sin^2\pi st/(\pi st)^2$ only becomes really noticeable for $t>0{\cdot}05\ \bar{X}$ and is then more marked in the higher orders. In all cases, expressions (6) to (9) tend to break down when the peaks become so broad that they merge with their neighbours. Nevertheless in these circumstances I_n as given by equation (7) has still been found to be representative of the mean intensity around the point $s\bar{X}=n$.

Interpretation of peak intensities when t > 0

The above analysis shows that the position and width of the diffraction peaks are essentially unaffected by the value of t. The only noticeable effects are on the integral intensities of the peaks. It is the purpose of this section therefore to examine how deductions from integral intensity measurements will be modified when a structure is interpreted in terms of a trapezium model with $t>0$, instead of the simpler rectangle where $t=0$. To form a basis for discussion several quantities relevant to absolute and relative intensity measurements have been evaluated in Table 1 for various combinations of χ and t. It should be emphasized that the quantity I_B in this article is related to the diffraction of a point collimated beam from only one one-dimensional periodic structure. To compare with experimental curves one must multiply by the Lorentz factor associated with the orientations of all the structural units within the sample (Hosemann & Bagchi, 1962, p. 440), and also account for slit smearing if a line collimated beam is used (Kortleve & Vonk, 1968).

First consider experiments involving the absolute measurement of the total integral intensity and its interpretation with equation (8). In previous reports of such measurements (*e.g.* Fischer, Goddar & Schmidt, 1967; Hermans & Weidinger, 1960) it has been assumed that $t=0$; the experimental measurements have then been used to test the consistency between χ and ϱ_0 for a simple rectangle model. However, equation (8) shows that the total intensity is reduced by increasing t and furthermore, that the same value can be produced

by various combinations of χ and t. The size of the effect is shown in the first column of the Table by the variation of the quantity $\{\chi(1-\chi)-\frac{1}{3}(t/\bar{X})\}$. Thus it is possible to introduce systematic errors into the interpretation by *a priori* assuming an incorrect value of t for the structure. However errors can also be introduced into this type of experiment due to the limitations and difficulties of measuring low intensity levels. With present equipment and using the most ordered sediments of polymer crystals, only the first three peaks can be detected with any certainty and accurate intensity measurements are usually only available for the first two. (In the published intensity curve of Fischer, Goddar & Schmidt (1967), the fourth diffraction peak is only just visible.) However, if the results are to be interpreted with equation (8), all of the scattered intensity must be measured; if this is not done a further systematic error will be introduced. By comparing equation (7) with equation (8) it is possible to estimate how the individual peaks contribute to the total intensity. For example when $\chi=0{\cdot}85$ and $t=0$, it is found that I_1 contributes 32·7%, I_2 gives 26·0%, I_3 gives 17·15% and I_4 gives 8·9%. Thus even if one optimistically assumes that all the intensity of the first four peaks can be detected, the measured intensity will in this example only represent 85% of that predicted by equation (8). The second column of Table 1 shows how the percentage in the first four peaks varies with χ and t. When $t=0$ about 12–15% of total predicted scatter is neglected, whereas when $t=0{\cdot}1\ \bar{X}$ only 1–2% is neglected. However the actual proportion neglected in a particular case will depend on both the values of t and on the position of the experimental cut-off. Attempts can be made to compensate for the neglected scatter by assuming that the tail of I_B where the intensity becomes indistinct will fall off with a $1/s^2$ dependence (Kortleve & Vonk, 1968). Although this procedure can be justified for a sharp two phase structure with $t=0$, the eventual fall-off for $t>0$ will be faster than this.

In the above experiments, the measurement of the intensity and the effects of t, both become more problematic with larger scattering angles. These difficulties can be minimized by restricting the measurement to only the first order peak and interpreting the results with equation (7). The third column of Table 1 shows I_1/ϱ_0^2; it is seen to be sensitive to changes in χ but very insensitive to t. For reasonable values of t, I_1 will remain essentially unchanged from its value at $t=0$. Hence provided the peak can be separated from the background and neighbouring peaks, this method is better than measuring the whole intensity curve in that it enables ϱ_0 and χ to be related without any ambiguity from the unknown value of t.

Finally consider the measurement of relative intensities. Due to the practical difficulties with higher order peaks and to the general degree of disorder in most samples, it is likely that only R_2 will be resolvable. The variation of R_2 is shown in the last column of Table 1. R_2 is mainly affected by χ and it is relatively insensitive to t. If this small change with t is acceptable and can be ignored, it is evident that for the purpose of correlating the scatter with χ a measurement of R_2 can be a valuable alternative to, or complement to, the measurement of I_1, especially as R_2 does not involve ϱ_0. It is interesting to note that if in calculating χ from I_1 and R_2, the parameter t is wrongly made zero then I_1 will give a slight overestimate of χ, while R_2 will give an underestimate.

In principle if sufficient peaks can be resolved and accurately measured, t as well as χ can be determined by elimination from equations (7) and (9). Unfortunately in practice the range most sensitive to changes in t is over the third and higher order peaks, where the intensity is low and difficult to measure. It is therefore likely to be impractical to estimate t with any accuracy. However even if t were to be determined for a particular polymer sample, it would only be immediately significant as a parameter in the one dimensional model. The main challenge would be to interpret the distance of transition in terms of a projection of the molecular structure within the sample.

Summarizing, the possibility of a finite but unknown transition length introduces an uncertainty into deductions involving χ. The effect is most serious with intensity measurements which involve the higher order peaks, such as measurements of the total scattered intensity. If however the measurements are restricted to just the first order peak the error becomes very small and one can interpret the results using a simple rectangle model irrespective of whether or not an effective transition zone is present.

References

BASSETT, G. A., BLUNDELL, D. J. & KELLER, A. (1967). *J. Macromol. Sci. (Phys.)*, B**1**, 161.

BLUNDELL, D. J. (1969). *Acta Cryst.* A**26**, 472.

Table 1. *Variation of some quantities related to intensity*

Model parameters		$[\chi(1-\chi)-\frac{1}{3}(t/\bar{X})]$	Percentage of intensity in first	I_1/ϱ_0^2	R_2
χ	$t/\bar{X}$	[see equation (8)]	four peaks	[see equation (7)]	[from equation (9)]
0·75	0	0·187	87	0·0506	0·500
0·75	0·1	0·154	98	0·049	0·453
0·8	0	0·160	88	0·035	0·653
0·8	0·1	0·127	99	0·034	0·593
0·85	0	0·127	85	0·0209	0·795
0·85	0·1	0·094	98	0·0202	0·720

DEBYE, P., ANDERSON, H. R. JR & BRUMBERGER, H. (1957). *J. Appl. Phys.* **28**, 679.
FISCHER, E. W., GODDAR, H. & SCHMIDT, G. F. (1967). *J. Polymer Sci.* B5, 619.
FRANK, F. C. & TOSI, M. (1961). *Proc. Roy. Soc.* A263, 323.
HERMANS, P. H. & WEIDINGER, A. (1960). *Makromol. Chem.* **39**, 67.
HOSEMANN, R. (1949). *Z. Phys.* **127**, 16.
HOSEMANN, R. (1967). *J. Polymer Sci.* C, **20**, 1.
HOSEMANN, R. & BAGCHI, S. N. (1962). *Direct Analysis of Diffraction by Matter*. Amsterdam: North Holland.
HOSEMANN, R., WILKE, W. & BALTA CALLEJA, F. J. (1966). *Acta Cryst.* **21**, 118.
KELLER, A. (1968). *Rep. Progr. Phys.* **31**, 623.
KORTLEVE, G. & VONK, C. G. (1968). *Kolloid-Z.* **225**, 124.
LINDENMEYER, P. H. & HOSEMANN, R. (1963). *J. Appl. Phys.* **34**, 42.
POROD, G. (1951). *Kolloid-Z.* **124**, 83.
POROD, G. (1952). *Kolloid-Z.* **125**, 51.
RHEINHOLD, C., FISCHER, E. W. & PETERLIN, A. (1964). *J. Appl. Phys.* **35**, 71.
TSVANKIN, D. YA. (1964*a*). *Vysokomol. Soyed.* **6**, 2078.
TSVANKIN, D. YA. (1964*b*). *Vysokomol. Soyed.* **6**, 2083.
WILLIAMS, T., BLUNDELL, D. J., KELLER, A. & WARD, I. M. (1968). *J. Polymer Sci.* A2, **6**, 1613.
ZERNIKE, F. & PRINS, J. A. (1927). *Z. Phys.* **41**, 184.

Acta Cryst. (1970). A**26**, 483

Diffuse X-ray Scattering from Crystals of Hexamminecobalt(III) Nitrate

By H. GOWDA, R. L. BANERJEE* AND R. O. W. FLETCHER

Physics Division, College of Arts & Science, University of the West Indies, St. Augustine, Trinidad

(*Received* 10 *April* 1969 *and in revised form* 2 *January* 1970)

Crystals of hexamminecobalt(III) nitrate are found not to be cubic like those of the thiocyanatopentammine derivative but to be tetragonal and of space group symmetry $P4_2nm$. The unit-cell parameters are $a=b=21{\cdot}66$, $c=33{\cdot}32\pm0{\cdot}05$ Å. The most prominent feature of the difference in response to X-rays of these and similar crystals is the heavy diffuse scattering produced by the hexamminecobalt(III) nitrate. By means of a series of cylindrical Laue photographs, taken with monochromatic cobalt (Co $K\alpha$) radiation, covering a quadrant of reciprocal space at regular intervals of 5° about the tetragonal axis, the diffuse domains in the reciprocal lattice are explored and information obtained on the nature and direction of propagation of the thermal waves in the crystal. An interesting feature of the crystal dynamics of hexamminecobalt(III) nitrate is that the only effects observed as a result of independent motion of large structural units are those of transverse waves. There are no noticeable similar effects ascribable to longitudinal waves. Thus information is obtained on the behaviour, shape and orientation of the structural units $[Co(NH_3)_6]^{3+}$ and $(NO_3)^-$.

Introduction

It has been observed by Fletcher & McDoom (1967) that in the crystal of the inorganic salts of the hexammine and pentammine complexes of cobalt and related metals the symmetry of each crystal depends on (i) the effective symmetry of the complex cation, and (ii) the nature and symmetry of the anion or anionic components. On the basis of a study of the X-ray diffraction spectra, they suggested further that in the cubic crystals of aquopentamminecobalt(III) perchlorate $[Co(NH_3)_5.H_2O](ClO_4)_3$ the complex ion $[Co(NH_3)_5.H_2O]^{3+}$ exhibits ellipsoidal rotation.

This is consistent with the report by Hassel & Bödtker Naess (1928) that these crystals as well as those of hexamminecobalt(III) perchlorate

$$[Co(NH_3)_6](ClO_4)_3$$

are cubic.

However, in the case of hexamminecobalt(III) nitrate $[Co(NH_3)_6](NO_3)_3$ and its monosubstituted thiocyanato derivative $[Co(NH_3)_5NCS](NO_3)_2$, the former is not cubic while the latter is. The symmetry of the crystals of the hexammine compound has been found, as will be described presently, to be tetragonal and that of space group $P4_2nm$; while that of the corresponding thiocyanatopentammine compound was determined (though not reported) by Price & Fletcher (1965), and confirmed in the course of these investigations to be cubic and that of space group $Fm3m$.

Moreover, one of the most distinctive features of the response to X-rays of these crystals and others being studied in this laboratory is the heavy diffuse scattering produced by the crystals of hexamminecobalt(III) nitrate, as opposed to the others.

It has been shown by Laval (1938, 1939*a*,*b*) and Lonsdale (1942, 1942-3), and others, that the diffuse scattering produced by simple crystals is essentially of thermal origin resulting from the vibrations of the individual atoms or monatomic ions; and is of two types, appearing on photographs as: (i) spots and (ii) streaks, whose maxima in both cases are always found to be on the unforbidden reciprocal lattice points.

* Present address: Department of Physics, University of Moncton, Moncton, N.B., Canada.